

1 **OVGP1 is an oviductal fluid factor essential particularly for early**
2 **embryonic development in golden hamsters**

3 **Running title:** *Ovgp1*-knockout hamsters

4 Kenji Yamatoya^{1*}, Masaru Kurosawa^{1*}, Michiko Hirose², Yoshiki Miura³,

5 Hikari Taka³, Tomoyuki Nakano⁴, Akiko Hasegawa⁵, Kyosuke Kagami⁶,

6 Hiroshi Yoshitake¹, Kaoru Goto⁴, Takashi Ueno³, Hiroshi Fujiwara⁶, Yoichi Shinkai⁷,

7 Frederick W. K. Kan⁸, Atsuo Ogura², Yoshihiko Araki^{1,9,10#},

8 ¹Institute for Environmental & Gender-specific Medicine, Juntendo University Graduate
9 School of Medicine, Chiba, Japan; ²RIKEN BioResource Research Center, Ibaraki,
10 Japan; ³Laboratory of Proteomics & Biomolecular Science, Biomedical Research Core
11 Facilities, Juntendo University Graduate School of Medicine, Tokyo, Japan;
12 ⁴Department of Anatomy and Cell Biology, Yamagata University School of Medicine,
13 Yamagata, Japan; ⁵Department of Obstetrics & Gynecology, Hyogo Medical University,
14 Hyogo, Japan; ⁶Department of Obstetrics & Gynecology, Kanazawa University
15 Graduate School of Medical Sciences, Ishikawa, Japan; ⁷Cellular Memory Laboratory,
16 RIKEN Cluster for Pioneering Research, RIKEN, Saitama, Japan; ⁸Department of
17 Biomedical and Molecular Sciences, Faculty of Health Sciences, Queen's University,
18 ON, Canada; ⁹Department of Obstetrics & Gynecology, Juntendo University Graduate

19 School of Medicine, Tokyo, Japan; ¹⁰Division of Microbiology and Immunology,
20 Department of Pathology and Microbiology, Nihon University School of Medicine,
21 Tokyo, Japan.

22 **These authors have contributed equally to this study.

23 #Correspondence:

24 Yoshihiko Araki

25 30-1 Oyaguchi-Kamicho, Itabashi-ku, Tokyo 173-8610, Japan

26 Tel: +81-3-3972-8111 ext.2261 E-mail yaraki@juntendo.ac.jp

27 **Keywords:** oviductal glycoprotein 1 (OVGP1); knockout-hamster; infertility;

28 early developmental failure; embryonic lethality

29 **Author contribution statement**

30 KY and MK designed the study, collected data, performed data analysis, and provided
31 financial support. HY designed and supervised the study, and provided financial
32 support. MH and AO generated *Ovgp-1* deficient hamsters and provided financial
33 support. YM, HT, TN, AH, KK, KG, YS and TU collected data and performed data
34 analysis/interpretation. HF and AO analyzed the data, provided financial supports. YA
35 and FWKK conceived, designed and directed the study, provided financial support and
36 wrote the article. All authors have given approval to the final version of the article.

37 **Abstract**

38 The mammalian oviductal lumen is a specialized chamber that provides an environment
39 that strictly regulates fertilization and early embryogenesis, the regulatory mechanisms to
40 gametes/zygote are still largely unknown. In this report, we studied the oviductal
41 regulation of early embryonic development using *Ovgp1* (a gene encoding an oviductal
42 humoral factor, OVGPI)-knockout (KO) hamsters. The experimental results revealed
43 the following: 1) Female *Ovgp1*-KO hamsters fail to produce any litters at all; 2) In the
44 oviducts from KO animal, fertilized eggs are sometimes identified, but their
45 morphology shows abnormal features; 3) The number of implantations in the KO
46 females is evidently low; 4) Even if implantations occur, the embryos develop
47 abnormally and eventually become embryonic lethal; and 5) *Ovgp1*-KO females
48 transferred to wild-type females produce KO egg-derived litters, but the reverse
49 experiment does not. These results suggest that OVGPI-mediated physiological events
50 are crucial for early embryonic development *in vivo*. This animal model shows that the
51 fate of the fertilized egg is not only genetically determined, but that the surrounding
52 oviductal microenvironment plays a pivotal role in normal embryonic development.

53

54 **Summary statement**

55 Deficiency an oviductal humoral factor (OVGP1) caused female infertility in the

56 golden hamsters. The presence or absence of OVGP1 has significant physiological

57 effects on early embryonic development *in vivo*.

58 **Introduction**

59

60 The mammalian oviduct is an intra-abdominal organ that serves as the site of
61 fertilization and early embryonic development prior to implantation of the blastocysts in
62 the endometrium. The lumen of the oviduct where fertilization takes place is strictly
63 extracorporeal, as is the lumen of the gastrointestinal tract. Thus, the mammalian
64 reproductive process from fertilization to preimplantation is essentially an "*ex vivo*"
65 event. Because mammalian fertilization appears to take place inside the body, *in vitro*
66 fertilization (IVF), the current treatment method in infertility medicine, is generally
67 misunderstood as a special type of fertilization, but the fact that it takes place outside
68 the body does not make it a special fertilization condition.

69 The use of culture medium with a clearly defined composition in mammalian IVF
70 was pioneered by Yanagimachi and Chang using the golden hamster (*Mesocricetus*
71 *auratus*) as an animal model [Yanagimachi & Chang, 1964]. This technique was
72 originally developed to visualize mammalian fertilization. Since then, the theory
73 developed has evolved into an important and fundamental principle for the development
74 of human IVF methods [Edwards et al. 1969]. As a treatment for infertility,
75 especially in humans, IVF-embryo transfer (ET), in which oocytes are harvested

76 directly from the ovaries without passing through the Fallopian tubes (oviducts),
77 fertilized, and cultured in test tubes (dishes), then transferred vaginally into the uterine
78 cavity, has become widely used worldwide. Therefore, oviductal factors are generally
79 considered not always necessarily in the IVF-ET process, and studies of the
80 reproductive physiology of the oviducts have been neglected as a worldwide trend,
81 especially during the last two decades. However, the oviduct (or its homologous organ),
82 the original site of fertilization and early embryonic development, is widely conserved
83 in lower vertebrates as well as in mammals. The origin of sexually reproducing
84 organisms can be traced back to the Cambrian period, at least 600 million years ago
85 [Araki et al, 2021; Araki 2022]. The physiological functions of the oviduct, which have
86 been widely conserved during the long process of evolution and selection, are naturally
87 thought to have important functions (not necessarily one) which are not yet known.

88 The medium for IVF-ET has a long history of development based on the composition
89 of the original Fallopian tube and uterine fluids [Quinn et al, 1985ab; Gardner et al,
90 1996]. The composition was based on the concentrations of glucose, inorganic salts,
91 growth factors and hormones, but at that time the proteins, which are the main
92 components of oviductal fluid, were largely unknown. Therefore, serum components
93 were used as a substitute for the other components of the oviductal fluid. However,

94 the ultimate goal of IVF should be to reproduce the *in vivo* oviductal microenvironment
95 as closely as possible, as a medical treatment. It is also biologically important to
96 elucidate the reproductive physiology of the oviduct, or the site of fertilization and early
97 embryonic development in the majority of mammals.

98 In this study, using the golden hamster as a prototype model for mammalian IVF, we
99 have provided evidence to demonstrate that a humoral factor in the oviduct, Oviductal
100 glycoprotein 1 (OVGP1) has a significant effect on early embryonic development *in*
101 *vivo*.

102 **Results**

103 **Generation of OVGP1-deficient hamsters**

104 Among oviductal factors identified in the oviductal fluid, OVGP1 has been well
105 characterized and suggested to play important roles in the process of several
106 mammalian species, including humans [for review, see Araki & Yoshida-Komiya,
107 1998; Buhi 2002; Avilés et al, 2010; González-Brusi et al, 2020; Zhao et al, 2022].
108 Using the golden hamster as a model, which has provided a wealth of knowledge
109 concerning the mammalian reproductive process [Hirose & Ogura, 2019], *Ovgp1*-
110 knockout (KO) animals were generated using gene editing technology (Suppl. Fig.
111 1A,B). Preliminary mating experiments showed that the F0 KO females (2 independent
112 individuals; #8, #10) did not produce any offspring. On the other hand, KO males (#3,
113 #4) were found to be as fertile as those of wild-type (WT). In the F1 and later
114 generations, fertility was confirmed in 17 of 23 (73%) KO male individuals. Fertility
115 was also confirmed to be possible in heterozygous females; 28 of 45 (62%)
116 heterozygous-female individuals were confirmed fertile with an average litter size of
117 7.08, in the post-F1 generation. Therefore, we maintained a line of KO males and
118 heterozygous females for further experiments.

119 Western blotting with OVGP1-specific antibodies did not reveal OVGP1 expression
120 signal in *Ovgp1*-KO hamster oviducts (Suppl. Fig. 1C). In additional mating
121 experiments with F0-F2 KO females with WT males with confirmed fertility (total pair
122 number: 15), no litters were obtained from all *Ovgp1*-KO females (Suppl. Fig. 2A).
123 These results suggest a lack of fertility in *Ovgp1* KO females. However, a F0 female
124 (#10) used in the mating experiment did not show any outward signs of pregnancy, but
125 went into shock and died suddenly at 15-day-post-coitus (dpc)(almost full-term) after
126 several mating sessions (Suppl. Fig.2B). An autopsy revealed that the death was almost
127 sudden, as there was a large amount of food in the gastrointestinal tract. Both uterine
128 horns were externally hematomatous, and the split surface had a hematoma visible to
129 the naked eye around the fetal sac, but no fetus was observed (Suppl. Fig. 2Ba; 2Bb).
130 After fixation, observation under a light microscope revealed a placenta-like structure,
131 but no fetal scar was noticeable due to absorption and hemorrhage (Suppl. Fig. 2Bc).
132 Since this phenomenon was limited to this one case and was an F0 individual, we
133 cannot conclude at this time that it was the result of *Ovgp1* gene editing. However, this
134 was considered a clear example of how OVGP1 may have a significant effect on the
135 reproductive process in the hamster models.
136

137 **Fertilizing ability of *Ovgp1*-KO females**

138 In order to find out what happened during the reproductive process, we first went on
139 to examine the development of the eggs after mating. In *Ovgp1*-KO animals, some
140 of the 1-dpc eggs appeared to be fertilized, but not most as in WT (Fig. 1A (control), D).
141 When examined under the light microscope (binary image), the egg cytoplasm from the
142 KO hamsters showed a central accumulation of intracellular organelles (Fig. 1B
143 (control), E). Electron microscopy showed that the KO eggs at 1-dpc displayed a
144 thinner zona pellucida (ZP) and a heterogeneous distribution of intracellular organelles
145 (Fig. 1C (control), F). In contrast to the synchronous development of four to eight cells
146 in fertilized eggs in WT 2.5-dpc, eggs in the oviducts of *Ovgp1*-KO females showed
147 developmental abnormalities evident at the level of light microscopy, such as delayed
148 development, disproportionate egg breakage and degeneration (Suppl.Fig.3).

149 At 4.5-dpc, implantation sites were observed in WT animals but not in the KO
150 animals (Fig. 2A). At the time of this experiment, it was thought that early embryos
151 might not implant in *Ovgp1*-KO female animals. However, at 5.5-dpc, statistically
152 significant fewer implantation sites were observed in the KO hamsters (Fig. 2B). These
153 results suggest that at least a small number of embryos produced by the KO females
154 were able to implant in the uterus.

155

156 **Histological findings of 8.5-dpc embryos of *Ovgp1*-KO females**

157 At 8.5-dpc, WT implanting embryos were well developed and pregnancy was clearly
158 visible (Fig. 3A-a). On the contrary, in *Ovgp1*-KO females, the number of implanting
159 embryos at 7.5-8.5-dpc was small or not well visible to the naked eye (n=4). Among
160 them, one individual appeared to be as well developed in appearance as those of the WT
161 (Fig, 3A-b).

162 The uterine epithelium of *Ovgp1*-KO hamsters (non-pregnant) showed no obvious
163 abnormality under the light microscope (Fig. 3B) when compared to the uterine
164 epithelium of WT hamsters. At 8.5-dpc of WT, the embryo was well developed and the
165 developing embryo and placenta can be seen in the fetal sac (Fig.3C). The developing
166 embryo (fetus) can be seen with the naked eye. The endometrium, except for the
167 implantation sites, can be seen to be composed of single columnar epithelium (Fig. 3C,
168 inset).

169 In *Ovgp1*-KO hamsters, no developing fetus was observed either with the naked eye
170 or under the stereomicroscope. When examined under a light microscope,
171 placenta/decidua-like primordial tissue with hemorrhagic degeneration was observed,
172 but no trace of embryo buds could be seen, and there was marked hemorrhage in the

173 placenta and uterine cavity (Fig.3D, arrowheads). It should be noted that the
174 endometrium adjacent to the implantation site differed from that of the WT in that it
175 showed formation of epithelial folds reminiscent of the ampulla of the oviduct (Fig.3D,
176 arrows). High magnification of this area revealed the presence of numerous cuboidal
177 cells each with a spherical nucleus and pale cytoplasm (Fig.3D, inset, noted by
178 asterisks). These are probably secretory cells intercalating with non-secretory cells
179 reflective of the typical columnar epithelium found in the WT.

180

181 **Validation of phenotypic recovery after ovarian transplantation**

182 Female hamsters in which the *Ovgp1* coding region was inactivated by gene editing
183 became completely infertile. This is strongly suggested to be the result of the absence
184 of OVGP1 in the oviductal microenvironment of the KO female hamsters, which
185 adversely affects early embryonic development immediately after fertilization.
186 However, in order to confirm that this clear phenotype is correct, it is usually necessary
187 to knock-in the inactivated gene region and see if the phenotype is restored. At present,
188 however, there are technical limitations to achieve this in hamsters, since they have
189 more fragile eggs than mice. Instead, we tried to see if we could restore the phenotype
190 using the ovarian transplant technique (Fig.4).

191 The fact that *Ovgp1*-KO male hamsters are fertile as described above, indicates that
192 even if the genotype of the zygote is *Ovgp1*^{+/-}, the embryo can develop normally and
193 produce litters in the wild-type oviduct microenvironment (Fig.4Aa). On the other hand,
194 embryos in the *Ovgp1*-KO female oviducts are lethally altered and no viable offspring
195 are produced whether the eggs are genotyped *Ovgp1*^{+/-} or ^{-/-} (Fig.4Ab).

196 What happened when these WT females were implanted with KO ovaries and mated
197 with KO males (Fig. 4Ac)? As expected, these experiments resulted in *Ovgp1*^{-/-} litters
198 (out of a total of 26 transplant experiments, litters were obtained from 11 individuals)
199 that could never be obtained by normal mating (Supple. Table S1; Fig.4B). These
200 litters can only be obtained under natural conditions by mating *Ovgp1*^{-/-} males with
201 *Ovgp1*^{+/-} females. Conversely, transplantation of the ovaries from WT individuals into
202 KO females did not result in any offspring (n=5): it is noteworthy to mention that
203 preliminary experiments of ovarian transplantation using WT females as both recipients
204 and donors, showed that 11 out of 14 (78.6%) transplanted animals produced litters.
205 The possibility that an individual transplanted with ovaries from a WT individual to a
206 KO female could produce litters cannot be ruled out. However, when ovarian
207 transplants were performed using a 78.6% success rate technique, no litters were

208 produced from all five individuals. The probability of such an event occurring can be
209 calculated to be less than 1%.

210

211 **What's going on in the *Ovgp1*-KO hamster oviduct: comprehensive**
212 **quantitative protein analysis in the oviduct after ovulation**

213 As noted above, OVGP1 is strongly suggested to be a microenvironmental factor in
214 the hamster oviduct, the site of fertilization and early embryonic development, with
215 pronounced effects on gametes and zygotes.

216 At this time, it is unclear whether the results obtained in the present study regarding
217 the physiological activity of OVGP1 is commonly found in other mammals. However,
218 at the very least, exploring what is happening in the hamster oviduct represents an
219 important first step toward understanding the molecular mechanisms of these
220 phenomena. Therefore, an attempt was first made to perform a comprehensive protein
221 microanalysis by confining the target especially to the oviduct with unfertilized eggs
222 retained immediately after ovulation in their lumen prior to mating.

223 Quantitative data for a total of 3,572 oviductal proteins were obtained by mass
224 spectrometry (MS) of the oviducts of super-ovulated animals (3 WT and 3 *Ovgp1*-KO,
225 each containing an unfertilized egg-cumulus complex in the oviduct lumen) (MS data

226 have been deposited in ProteomeXchange and jPOST with the accession
227 codes PXD037067 and JPST001867, respectively). In the Volcano diagram, changes
228 in the expression of oviductal proteins associated with OVGP1 deficiency were
229 observed. Of the 21 proteins that showed significant expression variation, a relatively
230 large number of down-regulated proteins (18 proteins) were identified, including some
231 the function of which has been previously implicated in the reproductive processes (Fig.
232 5; Supple. Table S2).

233 **Discussion**

234 This study has clearly shown, for the first time, that a deficiency of a fluid factor
235 secreted into the lumen of the oviduct causes lethal changes in early embryonic
236 development. Results of the present study are almost consistent with the currently
237 proposed bioactivities of OVGPI, which has been demonstrated in a variety of
238 mammalian models to date, including humans [Araki & Yoshida-Komiya, 1998; Buih
239 2002; Avilés et al, 2010; González-Brusi et al, 2020; Zao et al, 2022] summarized in
240 Figure 6. Although OVGPI has been suggested to be involved in sperm functions,
241 fertilization, and embryonic development, the clear KO phenotype observed in the
242 present study is a lethal change in embryonic development after fertilization. Since
243 normal embryonic development involves a comprehensive process including sperm-egg
244 function and fertilization, therefore, it is premature to conclude from this phenotype that
245 OVGPI is essential only for embryonic development.

246 In hamsters, OVGPI has been suggested to be an important fluid factor during *in*
247 *vivo* fertilization, especially since it modifies the ZP of oocytes in transit in the oviduct
248 after ovulation [Araki et al, 1987; Oikawa et al, 1988; Robitaille et al, 1988] and
249 inhibition of IVF was shown by targeting OVGPI with a specific antibody [Sakai et al,
250 1988]. However, the conditions of experiments *in vitro* carried out with OVGPI are

251 very different from their counterparts carried out *in vivo*, so that it is natural to argue
252 that we should be more cautious about evaluating *in vitro* interpretations as compared to
253 *in vivo* functions [O'Day-Bowman et al, 2002]. In addition, OVGPI has been found to
254 be taken up by the developing embryos after fertilizations [Kan et al, 1993], suggesting
255 that it may have a role in early embryonic development and may even have a function in
256 implantation [Roux et al, 1997]. The data obtained in the present study provide direct
257 evidence of the intrinsic importance of the physiological function of OVGPI in the
258 reproductive process of the hamster.

259 In considering the results of this study, it is necessary to reconsider the implications
260 of the lack of a clear phenotype in *Ovgp1*-KO mice published 20 years ago (these
261 genetically modified animals produced litters comparable to WT) [Araki et al, 2003].
262 At present, we cannot elaborate on the phenotypic differences between *Ovgp1*-KO mice
263 and hamsters due to insufficient experimental data. However, it is known that the
264 primary structure of OVGPI is highly conserved between species on the N-terminal end,
265 and that there is considerable structural diversity between species on the C-terminal end
266 and in its degree of glycosylation [Araki & Yoshida-Komiya, 1998; Zao et al, 2022].
267 Furthermore, until the end of the 20th century, the molecular characterization of
268 OVGPI was mainly carried out in large livestock such as cattle, pigs and sheep where

269 relatively large amounts of oviductal fluid were available, and in baboons as a human
270 model. Previous studies on the functions of OVGPI in the reproductive process have
271 been carried out in rodents using mainly hamsters, but not mice, because of the stability
272 of their sexual cycle. As for mouse OVGPI, there were only three reports all from the
273 same research group in the mid-1980s [Kapur & Johnson, 1985; 1986; 1988], and there
274 have been no further protein-level reports to date concerning mouse OVGPI. Since
275 the identification of OVGPI, knowledge about genetic engineering of mouse oviductal
276 glycoprotein has been accumulating [Sendai et al, 1995; Takahashi et al, 2000], while
277 studies of the underlying mechanisms of OVGPI that regulate its function are clearly
278 lacking. This is one of the reasons why research in this field has not progressed since
279 the establishment of the *Ovgp1*-KO mouse.

280 Elucidating the molecular mechanisms of the phenotype caused by OVGPI
281 deficiency is an urgent research priority. For this reason, the results of MS analysis
282 using oviducts immediately after ovulation (Fig. 5; Suppl. Table 2) could be one of the
283 breakthroughs. Among the group of molecules in the oviduct down-regulated by *Ovgp1*
284 KO hamsters, ZP3, the major component of ZP glycoproteins, deserves the first
285 attention. Although the importance of the ZP glycans and the structure and function of
286 homologous molecules among all animal models examined to date remains

287 controversial [Tulsiani et al, 1988; Moros-Nicolás et al, 2019; Tumova et al, 2021], ZP3
288 has been suggested to play an important role in fertilization due to the protein's three-
289 dimensional structure [Tracy et al, 1995; Han et al, 2010]. Similarly, serpin family E
290 member 2 (SERPIN2) and ovostatin homolog (OVOS), serine protease inhibitors, were
291 identified as down-regulated molecules by *Ovgp1*-KO hamsters (Fig. 5). SERPIN2 is
292 abundantly expressed in granulosa cells although its function is unknown in humans
293 [THE HUMAN PROTEIN ATRAS; [https://www.proteinatlas.org/ENSG00000135919-](https://www.proteinatlas.org/ENSG00000135919-SERPINE2)
294 SERPINE2]. Furthermore, OVOS has also been identified in mouse uterine fluid
295 [Huang et al, 2019] and may also be present in oviductal fluid. These findings suggest
296 that since unfertilized eggs are surrounded by cumulus cells (*i.e.*, granulosa cells) in the
297 oviductal lumen, the decrease in SERPIN2 and OVOS may have caused a local increase
298 in protease activity, which in turn, affected ZP3 stability and decreased fertilization
299 rates. In hamsters, OVGPI modifies the ZP promptly after ovulation [Araki et al, 1987;
300 Oikawa et al, 1988; Robitaille et al, 1988], and its loss may directly or indirectly affect
301 the three-dimensional structure of the ZP by downregulating ZP3. The latter
302 speculation is also consistent with the thinning of the ZP immediately after fertilization
303 as shown by electron microscopy (Fig. 1F). In general, the current status of research on
304 hamster OVGPI is that various databases are still underdeveloped compared to those of

305 humans and mice. However, since this is a problem that will be resolved over time, we
306 believe that the present study has provided sufficient and novel results that could
307 considered as a breakthrough in OVGPI research.

308 Early mammalian development (even before the widespread use of recombinant
309 technology) has been studied mainly in the mouse model. This is because the
310 development of blastocysts is easier in media with a simpler chemical composition, but
311 this development process is much more complex in the *in vivo* situation in mammals. *In*
312 *vitro* culture of non-mouse embryos, including humans, still has some technical issues
313 to overcome such as two-cell block and blastocyst formation, and it took a long time to
314 solve these problems in hamsters through various innovations [Schini & Bavister, 1988].
315 Although it is now possible to culture hamsters to blastocysts and obtain litters by
316 embryo transfer [Seshagiri & Vani, 2019], the unfertilized eggs used in these
317 experiments, whether in hamsters or mice, are usually prepared from oviducts after
318 ovulation. These facts suggest that the microenvironment in the oviduct and uterus,
319 which is generally important for early embryonic development, is governed by a variety
320 of cell biological control mechanisms. The *in vivo* interaction between the early
321 embryos and the epithelium of the female reproductive tract can be inferred from the
322 fact that early embryos, which are undifferentiated totipotent cells, have a much higher

323 mitotic potential than cancer cells (it is almost unlikely that a single cancer cell will
324 grow to the same weight as fetal tissue in the same amount of time as its gestation
325 period, not to mention the human example), and are reliably regulated to carry out
326 normal development.

327 At present, IVF-ET is widely used as a treatment for infertility in which eggs from
328 the ovaries are fertilized in a culture medium and trans-vaginally transferred into the
329 uterine cavity for subsequent implantation, but the reproductive physiology of the
330 oviducts has been long neglected as described above. However, the oviducts (and their
331 homologous organs), the original site of fertilization and early embryonic development,
332 are widely conserved in vertebrates as well as mammals, and one could imagine that
333 they have important physiological functions yet to be explored and unraveled. The
334 molecular comparison of the reproductive processes between the *Ovgp1*-KO hamsters
335 established in the present study and the homologous gene KO mice provides an
336 excellent animal model to further elucidate the mammalian reproductive mechanisms.

337 Comprehensive molecular dynamics studies are currently underway using these KO
338 animals. Future research originating from OVGp1 has the potential to elucidate some
339 aspects of the pathogenesis for human disease, such as infertility due to disorders of the

340 early fertilization process or infertility due to fetal growth retardation in the early stage

341 of pregnancy the causes of which remain unknown.

342 **Materials and Methods**

343 **Animals**

344 Sexually mature (7~8-week-old) golden hamsters (*Mesocricetus auratus*) were
345 purchased from Japan SLC, Inc. (Hamamatsu, Shizuoka, Japan). They were
346 maintained and bred at our Animal facilities under 12L:12D conditions. Observation of
347 sperms in the vaginal plug in females after mating was considered as 0-dpc. All animal
348 experiments were conducted according to the guidelines for care and use of laboratory
349 animals, Juntendo University (approval # 768) and RIKEN Tsukuba Institute, (approval
350 # T2021-Jitsu004) Japan.

351 For genotyping, ear biopsies were lysed with 0.4 mg/mL proteinase K (Nakalai
352 Tesque Inc., Kyoto, Japan) and partially purified using standard chloroform extraction.
353 Genomic fragments containing the target site were then amplified by PCR using primers
354 (forward: 5'-AAGCCAGAATCCAAAGCTGAAGCAC-3'; Reverse: 5'-
355 GTATTAAACCCTCACAACCTGGGCTC-3'). The PCR procedure followed the
356 instructions for Tks Gflex DNA polymerase (TaKaRa Bio Inc., Shiga, Japan). The
357 amplified PCR fragments were subcloned into the pGEM T Vector system (Promega
358 Corporation, Madison, WI, USA) and sequenced to confirm each allele.

359

360 **Generation of *Ovgp1*-KO hamsters**

361 *Ovgp1*-KO hamsters were established using an *in vivo* electroporation CRISPR–Cas9
362 system, essentially followed as described previously [Hirose et al, 2020]. Pairs of
363 sgRNAs were designed to delete the *OVGP1* genomic sequence from exon 1 to 3
364 (sequence of DNA targets: + allele; 5'-ACTGACTCCCTGCTAGCGTCAGG-3', -
365 allele; 5'-CCTGCTAGCGTCAGGCCACGGAT-3'; 5'-
366 CCATCGACCAGCCCCCTGAGCTG-3'; 5'- CCTCGATGACTTGGGAGTTAATG-
367 3')(Suppl. Fig.1A). Ten animals were born of which three male individuals (#1, 3, 4)
368 and two females individuals (#8, 10) appeared to be homozygously defective in the
369 target gene region (Suppl. Fig. 1B). Females #8 and #10 did not show any external signs
370 of pregnancy in mating experiments with wild-type males with confirmed fertility; two
371 males (#3, 4) were fertile and the defective gene was transmitted to their offspring when
372 mated with wild-type females. To minimize the possible effects of off-targeting when
373 heterozygotes were mated, two generations of heterozygotes were mated to wild-type
374 and the heterozygotes were mated to homozygous males derived from #3 and #4,
375 respectively, and were found to produce a normal number of offspring.

376

377 **Western blotting analysis**

378 The concentration of total protein extracted from animal organs was quantified using
379 BradfordUltra (Expedeon Ltd, Cambridgeshire, UK). Antibodies (Abs) specific for
380 hamster OVGPI used in this study were as follows: AZPO-8 (monoclonal Ab (mAb)
381 against the oligosaccharide portion of hamster OVGPI (mouse IgG1)[Araki et al,
382 1987]); anti-OVGPI N-terminal -peptide polyclonal Ab (pAb)(rabbit IgG, ab74544;
383 Abcam plc, Cambridge, UK); horse radish peroxidase (HRP)-conjugated anti-mouse
384 IgG pAb (P0260) and anti-rabbit IgG pAb (P0448)(Dako, Carpinteria, CA, USA).
385 Proteins were separated by SDS-PAGE system and transferred to Immobilon-P
386 membrane (Merck KGaA, Darmstadt, Germany). Immunoreactions were detected
387 according to standard methods described previously [Yoshitake et al, 2015; Oda-
388 Sakurai et al, 2019].

389

390 **Collection of eggs**

391 Eggs were collected from the oviducts of mature females by natural mating with
392 fertile males. Coitus was confirmed by the presence of vaginal sperm in the post-
393 ovulatory vaginal discharge and that day was defined as 0-dpc. For the collection of
394 unfertilized eggs in the oviduct, ovulation was artificially induced by gonadotropin
395 according to the standard method as described previously [Araki et al, 1987; 1992]

396

397 **Morphological observation**

398 Tissues from animals were fixed with 20% Formalin solution (FUJIFILM Wako
399 Chemical Co., Osaka, Japan) and embedded in paraffin wax according to standard
400 procedure. Three- μ m thick sections were cut and stained with Hematoxylin-Eosin for
401 light microscopic observations. For transmission electron microscopy, samples were
402 fixed with 2.5% glutaraldehyde (FUJIFILM Wako Pure Chemical) in 0.1 M phosphate
403 buffer (PB)(pH 7.2) followed by post-fixation with 2% OsO₄ in 0.1 M PB (pH 7.4).
404 Fixed specimens were dehydrated with a graded series of ethanol, and embedded in
405 Epok812 (Okenshoji Co., Ltd. Tokyo, Japan) according to standard procedure.

406 To detect implantation site(s), a solution of Chicago Sky Blue 6B (Tokyo Kasei
407 Kogyo Co., Ltd.) diluted to 1% in saline was injected into the heart of female animals
408 under anesthesia. After circulating for 10 min, blood was perfused with 50 mL of PB
409 saline to clearly visualize the blue pigment in the uterus.

410

411 **Ovary transplantation**

412 The technique of ovarian transplantation used in this study essentially followed the
413 methods reported elsewhere [Yun et al, 1990; Takahashi et al., 2001; Miyoshi et al,

414 2002].

415

416 **Statistical analysis**

417 To compare the implantation number at 5.5-dpc of WT and *Ovgp1* KO female
418 animals, the Mann-Whitney *U* test was utilized. A probability of $p < 0.05$ was
419 considered statistically significant.

420

421 **Quantitative protein MS analysis**

422 **a) Sample preparation and protein digestion**

423 Three oviducts collected at after ovulation induced by hormonal induction from each
424 of WT and *Ovgp1*-KO hamster were used for analysis. Samples were lyophilized and
425 stored at -80°C until use. Protein digestion on S-Trap[™] micro (ProtiFi, Huntington, NY,
426 USA) was performed according to the manufacturer's procedure, except for reductive
427 alkylation. Briefly, lyophilized samples were mixed with lysis buffer containing 5%
428 SDS, 4 mM tris (2-carboxyethyl) phosphine, 16 mM chloroacetamide, 50 mM
429 triethylammonium bicarbonate (TEAB)(Thermo Fisher Scientific Inc., Waltham, MA,
430 USA) boiled at 95°C for 5 min, and cooled to room temperature for 30 min. Afterward,
431 phosphoric acid was added to oviductal lysate to a final concentration of 1.2%, and then

432 six volumes of binding buffer containing 90% methanol, 100 mM TEAB were added.
433 The protein solutions were loaded to an S-Trap filter, spun at $4,000 \times g$ for 30 sec.
434 Then the filter was washed 3 times with 150 μL of binding buffer. Finally, 2 μg of MS
435 grade Trypsin Platinum (Promega, Madison, WI, USA) in 40 μL of digestion buffer
436 containing 50 mM TEAB was added into the filter and digested at 37°C for 16 h. To
437 elute peptides, three stepwise buffers were applied, with 40 μL each containing 50 mM
438 TEAB, 0.2% formic acid in water, and 50% acetonitrile. The peptide solutions were
439 pooled, lyophilized, and desalted with a GL-Tip SDB column (GL Sciences, Tokyo,
440 Japan).

441

442 **b) Liquid chromatography (LC)/MS analysis**

443 LC/MS analysis was performed using an Orbitrap Eclipse Tribrid mass spectrometer
444 equipped with FAIMS PRO coupled to an EASY-nLC 1200 system (Thermo Fisher
445 Scientific Inc.). Peptides were resuspended in a mixture of 0.1% formic acid and 2%
446 acetonitrile (v/v), and then loaded on a packed C18 column (15 cm, 3 μm , 75 μm i.d.,
447 Nikyo Technos Co.,Ltd, Tokyo, Japan). As mobile phases, 0.1% formic acid in water
448 was used for mobile phase A and a mixture of 0.1% formic acid and 90% acetonitrile
449 (v/v) for mobile phase B. Peptides were separated with a linear gradient of acetonitrile

450 from 2% to 35% (phase B) at 120 min at flow rate of 300 nL/min. The mass
451 spectrometer was operated in positive ionization mode, and the correction voltages on
452 the FAIMS Pro interface were set to -40V, -60V, and -80V, respectively. Data-
453 dependent acquisition (DDA) was performed using the following parameters. MS1
454 resolution was set at 60,000, and a maximum inject time was set to auto and scan range
455 from 350 to 1,800 *m/z*. During the tandem MS (MS/MS) scan, the linear ion trap
456 analyzer detects, and the precursor sets its intensity threshold at 5,000. For precursor
457 fragmentation in High-energy collisional dissociation (HCD) mode, a normalized
458 collision energy of 30% was used.

459 Protein identification and label-free quantification were performed using Proteome
460 Discoverer (PD)(ver. 2.5.0.400, Thermo Fisher Scientific Inc.). SEQUEST HT in PD
461 and MASCOT (Version 2.8.0, Matrix Science Inc.) were used as search engines, and all
462 raw files were searched against a *Mesocricetus auratus* (Syrian Golden hamster) protein
463 database in Universal Proteins Resource Knowledgebase (UniProtKB)(32,230 entries,
464 2022_02). Carbamidomethylation of cysteine was a fixed modification, while
465 acetylation of the protein N-terminus and oxidation of methionine were variable
466 modifications. Mass tolerances were set at 10 ppm and 0.8 Da for MS and MS/MS,
467 respectively. A false discovery rate (FDR) of 1% was applied to the analysis for both

468 peptide and peptide spectral match levels. Peaks were detected and integrated using the
469 Minora algorithm embedded in PD. Proteins were quantified based on unique and razor
470 peptides intensities. Normalization was performed based on the total protein amount.

471 **Acknowledgments**

472 We are indebted to Dr. Satoshi Hayakawa (Nihon University), Dr. Ichiro Miyoshi, Dr.
473 Shoichiro Kurata (Tohoku University), and Dr. Hiromi Yoshida-Komiya (Fukushima
474 Medical University) for both material and emotional support. The authors express deep
475 appreciations to Dr. Soichiro Kakuta (Juntendo University) and Dr. Kei Fukuda
476 (RIKEN) for their technical supports in using electron microscopy and designing
477 gRNAs, respectively. The excellent secretarial assistance of Ms. Keiko Fukuda
478 (Jundendo University) and Ms. Mari Enomoto (Nihon University) is gratefully
479 acknowledged.

480

481 **Competing interests**

482 The authors declare that there is no conflict of interest that could be perceived as
483 prejudicing the impartiality of the research reported.

484

485 **Funding**

486 This work was supported in part by Grants-in-Aid for Scientific Research
487 [17K19734/18KK0256/22K09648 to YA, 19K22681/21H04837/22K18396 to HF,
488 21K09503 to HY, 19H00456/20H01113/21H04279/22H04388 to MK, 20K09608 to

489 KY, 19H03151/19H05758 to AO from the Minister of Education, Culture, Sports,
490 Science & Technology, Japan, and a grant from Japan Science and Technology Agency
491 No. 19-191030923 to HF.

492

493 **Data availability**

494 Data for comprehensive protein quantitative analysis by mass spectrometry reported in
495 this paper have been submitted to the ProteomeXchange and jPOST with the accession
496 codes PXD037067 and JPST001867, respectively.

497 **References**

498

499 **Araki, Y.** (2022) Embryos, cancers, and parasites: potential applications to the study of
500 reproductive biology in view of their similarity as biological phenomena. *Reprod. Med.*

501 *Biol.* **21**, e12447. doi: 10.1002/rmb2.12447

502

503 **Araki, Y., Kurata, S., Oikawa, T., Yamashita, T., Hiroi, M., Naiki, M. and Sendo,**
504 **F.** (1987) A monoclonal antibody reacting with the zona pellucida of the oviductal egg

505 but not with that of the ovarian egg of the golden hamster. *J. Reprod. Immunol.* **11**,193-

506 208. doi: 10.1016/0165-0378(87)90057-x

507

508 **Araki, Y., Orgebin-Crist, M.C. and Tulsiani, D.R.** (1992) Qualitative
509 characterization of oligosaccharide chains present on the rat zona pellucida

510 glycoconjugates. *Biol. Reprod.* **46**, 912-919. doi: 10.1095/biolreprod46.5.912

511

512 **Araki, Y., Nohara, M., Yoshida-Komiya, H., Kuramochi, T., Ito, M., Hoshi, H.,**

513 **Shinkai, Y. and Sendai, Y.** (2003) Effect of a null mutation of the oviduct-specific

514 glycoprotein gene on mouse fertilization. *Biochem. J.* **374**, 551-557. doi:

515 10.1042/BJ20030466.

516

517 **Araki, Y. and Yoshida-Komiya, H.** (1998) Mammalian oviduct-specific glycoprotein:

518 Characterization and potential role in fertilization process. *J. Reprod. Dev.* **44**, 215-228.

519 doi:10.1262/jrd.44.215

520

521 **Araki, Y., Yoshitake, H., Yamatoya, K. and Fujiwara, H.** (2021) An overview of sex

522 and reproductive immunity from an evolutionary/anthropological perspective. *Immunol.*

523 *Med.* **44**, 152-158. doi:10.1080/25785826.2020.1831219

524

525 **Avilés, M., Gutiérrez-Adán, A. and Coy, P.** (2010) Oviductal secretions: will they be

526 key factors for the future ARTs? *Mol. Hum. Reprod.* **16**, 896-906. doi:

527 10.1093/molehr/gaq056

528

529 **Buhi, W.** (2002) Characterization and biological roles of oviduct-specific, oestrogen-

530 dependent glycoprotein. *Reproduction* **123**, 355-362. doi:10.1530/rep.0.1230355

531

- 532 **Edwards, R.G., Bavister, B.D. and Steptoe, P.C.** (1969) Early stages of fertilization
533 in vitro of human oocytes matured in vitro. *Nature* **221**, 632-635. doi:10.1038/221632a0
534
- 535 **Gardner, D.K., Lane, M., Calderon, I. and Leeton, J.** (1996) Environment of the
536 pre-implantation human embryo in vivo: Metabolite analysis of oviduct and uterine
537 fluids and Metabolite analysis of oviduct and uterine fluids and metabolism of cumulus
538 cells. *Fertil. Steril.* **65**, 349-353. doi: 10.1016/s0015-0282(16)58097-2
539
- 540 **González-Brusi, L., Algarra, B., Moros-Nicolás, C., Izquierdo-Rico, M.J., Avilés,**
541 **M. and Jiménez-Movilla, M.** (2020) A Comparative View on the Oviductal
542 Environment during the Periconception Period. *Biomolecules* **10**, 1690. doi:
543 10.3390/biom10121690.
544
- 545 **Han, L., Monné, M., Okumura, H., Schwend, T., Cherry, A.L., Flot, D., Matsuda,**
546 **T. and Jovine, L.** (2010) Insights into egg coat assembly and egg-sperm interaction
547 from the X-ray structure of full-length ZP3. *Cell* **143**, 404-415. doi:
548 10.1016/j.cell.2010.09.041.
549

- 550 **Hirose, M. and Ogura A.** (2019) The golden (Syrian) hamster as a model for the study
551 of reproductive biology: Past, present, and future. *Reprod. Med. Biol.* **18**, 34-39.
552 doi:10.1002/rmb2.12241
- 553
- 554 **Hirose, M., Honda, A., Fulka, H., Tamura-Nakano, M., Matoba, S., Tomishima, T.,**
555 **Mochida, K., Hasegawa, A., Nagashima, K., Inoue, K., et al.** (2020) Acrosin is
556 essential for sperm penetration through the zona pellucida in hamsters. *Proc. Natl. Acad.*
557 *Sci. USA.* **117**, 2513-2518. doi: 10.1073/pnas.1917595117 (Erratum in: (2020) *Proc.*
558 *Natl. Acad. Sci. USA.* **117**, 24601.)
- 559
- 560 **Huang, H.L., Li, S.C. and Wu, J.F.** (2019) A complex of novel protease inhibitor,
561 ovostatin homolog, with its cognate proteases in immature mice uterine luminal
562 fluid. *Sci. Rep.* **9**:4973. <https://doi.org/10.1038/s41598-019-41426-4>
- 563
- 564 **Kan, F.W., Roux, E. and Bleau, G.** (1993) Immunolocalization of oviductin in
565 endocytic compartments in the blastomeres of developing embryos in the golden
566 hamster. *Biol. Reprod.* **48**, 77-88. doi: 10.1095/biolreprod48.1.77
- 567

568 **Kapur, R.P. and Johnson, L.V.** (1985) An oviductal fluid glycoprotein associated
569 with ovulated mouse ova and early embryos. *Dev. Biol.* **112**, 89-93. doi: 10.1016/0012-
570 1606(85)90122-8

571

572 **Kapur, R.P. and Johnson, L.V.** (1986) Selective sequestration of an oviductal fluid
573 glycoprotein in the perivitelline space of mouse oocytes and embryos. *J. Exp. Zool.* **238**,
574 249-260. doi: 10.1002/jez.1402380215

575

576 **Kapur, R.P. and Johnson, L.V.** (1988) Ultrastructural evidence that specialized
577 regions of the murine oviduct contribute a glycoprotein to the extracellular matrix of
578 mouse oocytes. *Anat. Rec.* **221**, 720-729. doi: 10.1002/ar.1092210307

579

580 **Miyoshi, I., Takahashi, K., Kon, Y., Okamura, T., Mototani, Y., Araki, Y. and**
581 **Kasai, N.** (2002) Mouse transgenic for murine oviduct-specific glycoprotein promoter-
582 driven simian virus 40 large T-antigen: tumor formation and its hormonal regulation.
583 *Mol. Reprod. Dev.* **63**, 168-176. doi: 10.1002/mrd.10175

584

585 **Moros-Nicolás, C., Chevret, P., Jiménez-Movilla, M., Algarra, B., Cots-Rodríguez,**
586 **P., González-Brusi, L., Avilés, M. and Izquierdo-Rico, M.J.** (2021) New Insights
587 into the Mammalian Egg Zona Pellucida. *Int. J. Mol. Sci.* **22**, 3276. doi:
588 10.3390/ijms22063276
589
590 **Oda-Sakurai R., Yoshitake, H., Miura, Y., Kazuno, S., Ueno, T., Hasegawa, A.,**
591 **Yamatoya, K., Takamori, K., Itakura, A., Fujiwara, H., et al.** (2019) NUP62: the
592 target of an anti-sperm auto-monoclonal antibody during testicular development.
593 *Reproduction* **158**, 503-516. doi: 10.1530/REP-19-0333
594
595 **O'Day-Bowman, M.B., Mavrogianis, P.A., Minshall, R.D. and Verhage, H.G.**
596 (2002) In vivo versus in vitro oviductal glycoprotein (OGP) association with the zona
597 pellucida (ZP) in the hamster and baboon. *Mol. Reprod. Dev.* **62**, 248-256. doi:
598 10.1002/mrd.10091
599
600 **Oikawa, T., Sendai, Y., Kurata, S. and Yanagimachi R.** (1988) A glycoprotein of
601 oviductal origin alters biochemical properties of the zona pellucida of hamster egg.
602 *Gamete Res.* **19**, 113-122. doi: 10.1002/mrd.1120190202

603

604 **Quinn, P., Kerin, J.F. and Warnes, G.M.** (1985a) Improved pregnancy rate in human
605 in vitro fertilization with the use of a medium based on the composition of human tubal
606 fluid. *Fertil. Steril.* **44**, 493-498. doi: 10.1016/s0015-0282(16)48918-1

607

608 **Quinn, P., Warnes, G.M., Kerin, J.F. and Kirby, C.** (1985b) Culture factors affecting
609 the success rate of in vitro fertilization and embryo transfer. *Ann. N. Y. Acad. Sci.* **442**,
610 195-204. doi:10.1111/j.1749-6632.1985.tb37520.x

611

612 **Robitaille, G., St-Jacques, S., Potier, M. and Bleau, G.** (1988) Characterization of an
613 oviductal glycoprotein associated with the ovulated hamster oocyte. *Biol. Reprod.* **38**,
614 687-694. doi: 10.1095/biolreprod38.3.687. PMID: 2454136.

615

616 **Roux, E., Bleau, G. and Kan, F.W.** (1997) Fate of hamster oviductin in the oviduct
617 and uterus during early gestation. *Mol. Reprod. Dev.* **46**:306-317. doi:
618 10.1002/(SICI)1098-2795(199703)46:3<306::AID-MRD9>3.0.CO;2-T

619

- 620 **Sakai, Y., Araki, Y., Yamashita, T., Kurata, S., Oikawa, T., Hiroi, M. and Sendo F.**
621 (1988) Inhibition of in vitro fertilization by a monoclonal antibody reacting with the
622 zona pellucida of the oviductal egg but not with that of the ovarian egg of the golden
623 hamster. *J. Reprod. Immunol.* **14**, 177-189. doi: 10.1016/0165-0378(88)90068-x
624
- 625 **Schini, S.A. and Bavister, B.D.** (1988) Two-cell block to development of cultured
626 hamster embryos is caused by phosphate and glucose. *Biol. Reprod.* **39**, 1183-1192. doi:
627 10.1095/biolreprod39.5.1183
628
- 629 **Sendai, Y., Komiya, H., Suzuki, K., Onuma, T., Kikuchi, M., Hoshi, H. and Araki**
630 **Y.** (1995) Molecular cloning and characterization of a mouse oviduct-specific
631 glycoprotein. *Biol. Reprod.* **53**, 285-294. doi: 10.1095/biolreprod53.2.285
632
- 633 **Seshagiri, P.B. and Vani, V.** (2019) Enabling Hamster Embryo Culture System:
634 Development of Preimplantation Embryos. *Methods Mol. Biol.* **2006**, 45-61. doi:
635 10.1007/978-1-4939-9566-0_4.
636

637 **Takahashi, K., Sendai, Y., Matsuda, Y., Hoshi, H., Hiroi, M. and Araki Y.** (2000)

638 Mouse oviduct-specific glycoprotein gene: genomic organization and structure of the 5'-

639 flanking regulatory region. *Biol. Reprod.* **62**, 217-226. doi: 10.1095/biolreprod62.2.217

640

641 **Takahashi, E., Miyoshi, I. and Nagasu, T.** Rescue of a transgenic mouse line by

642 transplantation of a frozen-thawed ovary obtained postmortem. *Contemp. Top. Lab.*

643 *Anim. Sci.* **40**, 28-31. PMID: 11451392

644

645 **Rankin, T., Familari, M., Lee, E., Ginsberg, A., Dwyer, N., Blanchette-Mackie, J.,**

646 **Drago, J., Westphal, H. and Dean J.** (1996) Mice homozygous for an insertional

647 mutation in the *Zp3* gene lack a zona pellucida and are infertile. *Development* **122**,

648 2903-2910. doi: 10.1242/dev.122.9.2903

649

650 **Tulsiani, D.R., Yoshida-Komiya, H. and Araki, Y.** Mammalian fertilization: a

651 carbohydrate-mediated event. *Biol. Reprod.* **57**, 487-494. doi:

652 10.1095/biolreprod57.3.487

653

654 **Tumova, L., Zigo, M., Sutovsky, P., Sedmikova, M. and Postlerova, P.** (2021)

655 Ligands and Receptors Involved in the Sperm-Zona Pellucida Interactions in Mammals.

656 *Cells* **10**, 133. doi: 10.3390/cells10010133.

657

658 **Yanagimachi, R. and Chang, M.C.** (1963) Fertilization of Hamster Eggs in vitro.

659 *Nature* **200**, 281-282. doi: 10.1038/200281b0

660

661 **Yun, J.S., Li, Y.S., Wight, D.C., Portanova, R., Selden, R.F. and Wagner, T.E.**

662 (1990) The human growth hormone transgene: expression in hemizygous and

663 homozygous mice. *Proc. Soc. Exp. Biol. Med.* **194**, 308-313. doi: 10.3181/00379727-

664 194-43096.

665

666 **Yoshitake, H., Hashii, N., Kawasaki, N., Endo, S., Takamori, K., Hasegawa, A.,**

667 **Fujiwara, H. and Araki, Y.** (2015) Chemical characterization of N-Linked

668 oligosaccharide as the antigen epitope recognized by an anti-sperm auto-monoclonal

669 antibody, Ts4. *PLoS One* **10**, e0133784. doi: 10.1371/journal.pone.0133784

670

- 671 **Zhao, Y., Vanderkooi, S. and Kan, F.W.K.** (2022) The role of oviduct-specific
672 glycoprotein (OVGP1) in modulating biological functions of gametes and embryos.
673 *Histochem. Cell Biol.* **157**, 371-388. doi: 10.1007/s00418-021-02065-x

674 **Figure legends**

675 **Figure 1.** Morphological findings of zygotes at 1-dpc in hamsters. Female animals
676 were mated spontaneously with fertile WT males. Eggs were collected from the
677 ampullary region of oviduct, and counter-stained with 4',6-diamidino-2-phenylindole
678 solution (FUJI FILM Wako Chemicals) for light microscopic (LM) observation and
679 some were processed for electron microscopy (EM). The images show eggs from WT
680 female (A, B; binary image of A, C; transmission electron microscopic (TEM) image)
681 and *Ovgpl*-KO female (D, E; binary image of D, F; TEM image), respectively.
682 Pronuclei indicated by arrowheads and sperm tails are shown by double arrowheads in
683 the high magnification images (A', D'). Bars; 50 μm (LM); 10 μm (EM)

684 **Figure 2.** Observation of fetal implantation in the uterus of hamsters. At 4.5-dpc (A),
685 and 5.5-dpc (B). Female animals were mated spontaneously with fertile WT males, and
686 showed typical uterine appearance at 4.5-dpc and 5.5-dpc (b). Box-and-whisker
687 diagram of the number of implantations at 5.5-dpc (c). *P*-value was calculated by the
688 Mann-Whitney *U* test. * *P*<0.05

689 **Figure 3.** Morphological findings of the uteri at 8.5-dpc in hamsters. (A) Appearance of
690 the uteri in pregnancy; WT (a) and *Ovgpl*-KO (b). Bars: 10 mm. (B) Sagittal section of

691 the uterus of a KO hamster in non-pregnant state. The inset shows a magnified view of
692 the endometrium. Bar: 500 μm (inset: 50 μm). Sagittal sections of pregnant uteri and
693 their corresponding magnified images (insets) of WT (C); *Ovgp1*-KO (D). Dc: decidua
694 cells ; PL, placenta; F, fetus. dPL; hemorrhagic degenerated placental tissues, dDC ;
695 denatured decidualized membrane cells. Arrowheads indicate hemorrhage traces, and
696 arrows reveal endometrial folds not seen in WT. Cuboidal epithelial cells with
697 spherical nuclei and bright cytoplasm are shown by asterisks (inset). Bars: 500 μm (50
698 μm in insets).

699

700 **Figure 4.** Effects of OVGP1 on early embryogenesis. (A) Schematic of fertilized eggs
701 and oviductal epithelium in early development: Post-fertilization embryos and oviductal
702 epithelium in WT (a) and *Ovgp1*-KO (b) females mated with either WT, heterozygous
703 (*Ovgp1*^{+/-}) or KO male, and what happens if a WT female is implanted with an *Ovgp1*-
704 KO ovary and mated with an *Ovgp1*-KO male?(c). (B) Typical results of ovarian
705 transplantation experiments proposed in A-c showing the appearance of litters (a) and
706 their genotyping (b).

707

708 **Figure 5.** Volcano diagram showing the down/up-regulated oviductal proteins after
709 ovulation in WT/*Ovgp1*-KO females. Oviducts were isolated from each of three
710 independent WT/*Ovgp1* KO individuals. Dotted red lines indicate the fold-change (FC)
711 protein expression at 2 and -0.5, and p -value = 0.05, respectively. Blue/red dots show
712 the down/up-regulated proteins in the oviducts from *Ovgp1*-KO females. BCAT1;
713 branched-chain-amino-acid aminotransferase, B3GNT7; hexosyltransferase, CCDC114;
714 coiled-coil domain-containing protein 114, CD63; tetraspanin, CD74; HLA class II
715 histocompatibility antigen gamma chain isoform X2, CKAP5; cytoskeleton-associated
716 protein 5, COPG2; Coatomer subunit gamma-2, CUNHXORF38; uncharacterized
717 protein CXorf38 homolog isoform X1; EXOC3; exocyst complex component 3,
718 HMGCS1; hydroxymethylglutaryl-CoA synthase, HSP60; 60 kDa heat shock protein,
719 mitochondrial,
720 JCHAIN; immunoglobulin J chain, OVGP1; oviduct-specific glycoprotein 1, OVOS;
721 ovostatin homolog, PLA2G7; platelet-activating factor acetylhydrolase, PNLIPRP2;
722 triacylglycerol lipase, SERPIN2; glia-derived nexin (serpin family E member 2),
723 SERPINB11; serpin family B member 11, RAB3B/D; Ras-related protein Rab-3B/D,
724 RPRD2; regulation of nuclear pre-mRNA domain containing 2, ZP3; zona pellucida
725 sperm-binding protein 3. KRT90; keratin, type II cytoskeletal cochlear-like, is

726 considered a contaminant in sample preparation and is listed in Supplementary Table S2

727 but omitted in this figure.

728

729 **Figure 6.** Potential physiological activities of an oviductal humoral factor OVGPI

730 during early reproductive process as suggested by the present study. Previous *in vitro*

731 experiments have proposed that OVGPI secreted from the oviduct 1) modifies the egg,

732 2) also modifies the sperm, and 3) is incorporated into the early embryo. The present

733 study has demonstrated that OVGPI is an essential factor that aids fertilization and the

734 normal development of early embryos (totipotent cells) in the hamster model. ZP, zona

735 pellucida; PB, polar body ; MP, male pronucleus; FP, female pronucleus; ST, sperm

736 tail; ICM, inner cell mass; OCT, outer cell mass.

737 **Supplementary Figure 1.** Production of *Ovgpl*-null hamsters. Gene structure of
738 hamster *Ovgpl* and its editing strategy (A). The position of the gene sequence to be
739 removed from EXON 1 to 3 is indicated by vertical arrows and the position of PCR
740 primers for mutant detection is indicated by red arrows. Genotypes of F0 animals after
741 gene editing by PCR (B). The positions of the predicted PCR products relative to the
742 genomic DNA are indicated by arrowheads (WT) and double arrowheads (KO),
743 respectively. Male #1, 3, 4 and female #8, 10 were successfully gene edited as designed.
744 Male #1, females #8, and #10 did not produce pups, so males #3 and #4 were used to
745 maintain the strain. #4(F3) indicates that DNA extracted from a F3 generation female
746 derived from a #4 F0 male individual was used as the template. Western blotting
747 analysis using OVGPI-specific antibodies (C); Equal amounts of tissue protein solution
748 were detected by SDS-PAGE followed by OVGPI-specific antibodies (AZPO8,
749 recognizing carbohydrate moiety of the OVGPI (a); ab74544, recognizing the N-
750 terminal peptide of OVGPI (b)). lanes 1: ovary, 2: oviduct and 3: uterus, respectively.

751

752 **Supplementary Figure 2.** Reproductive ability of *Ovgpl*-KO hamsters. Fertility of
753 *Ovgpl*-KO female hamsters (A). Female WT (n=5) and *Ovgpl*-KO (n=15) mated with
754 fertility confirmed WT males. Autopsy image (B) of an F0 *Ovgpl*-KO female (15-dpc)

755 that died suddenly during a mating experiment. Appearance of the uterus (a), its cross-

756 sectional image (b) and hematoxylin-eosin stained image (c). Bar = 1 mm.

757

758 **Supplementary Figure 3.** Early embryos at 2.5-dpc. From oviduct of WT (A) and

759 *Ovgp1*-KO animals (B). Bars = 50 μ m.

760 **Supplementary Table S1** Fertility of female individuals after ovarian transplantation.

761 * After the ovaries were implanted, they were mated with male individuals to see if they

762 could produce litters.

763 ** In 11 deliveries obtained after ovarian transplantation, the genotype of the fetus

764 could not be confirmed in 5 cases due to maternal cannibalism immediately after

765 delivery. The remaining 6 deliveries yielded a total of 29 fetuses (mean litter size =

766 4.83), 19 of which were *Ovgp1*^{-/-}.

767

768 **Supplementary Table S2** List of proteins whose expression was changed after

769 ovulation between WT and *Ovgp1*-KO hamsters oviducts. Of the 3573 proteins

770 identified, 3/19 were significantly up/down regulated, respectively (these Volcano plots

771 are shown in Figure 5).

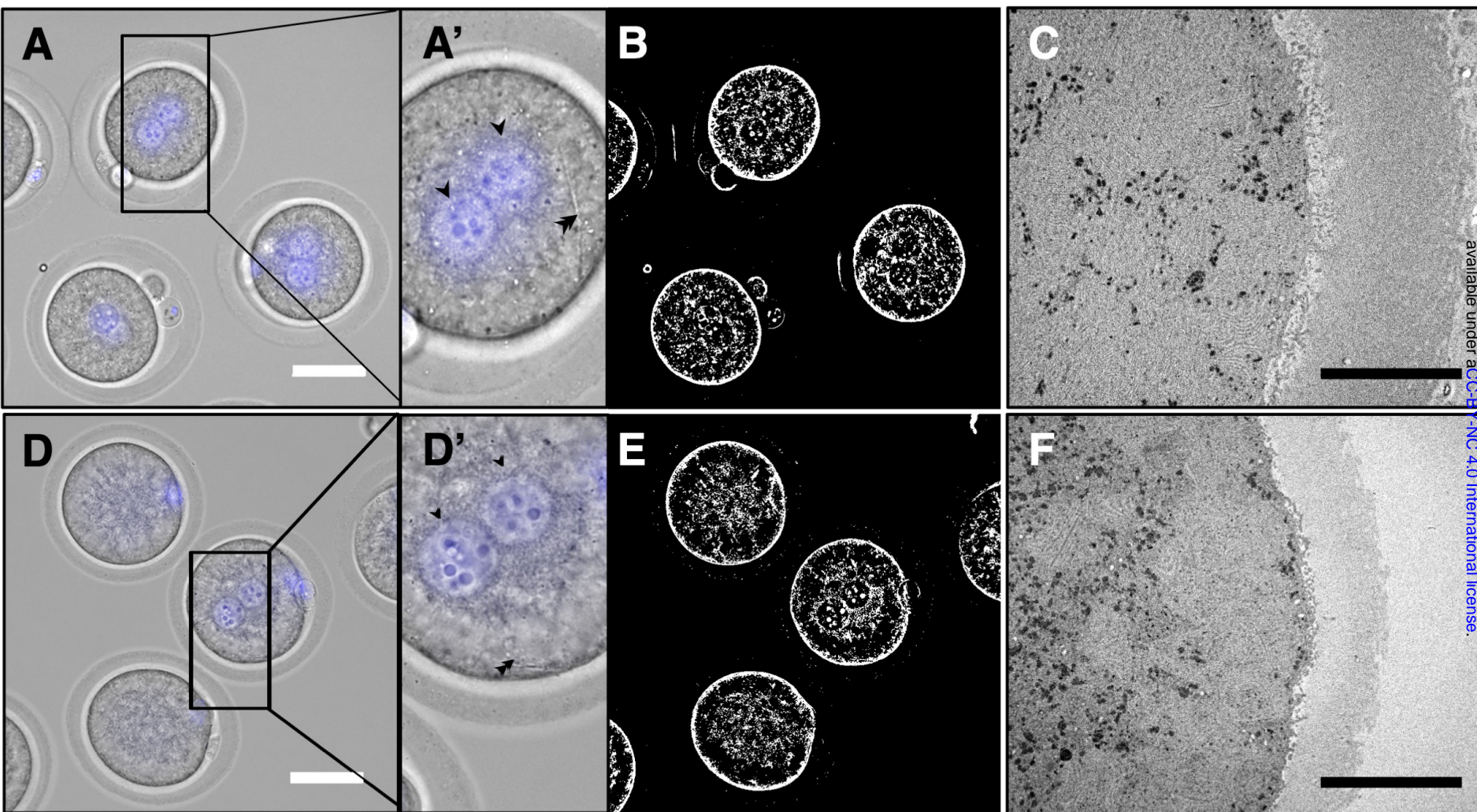


Figure 1.

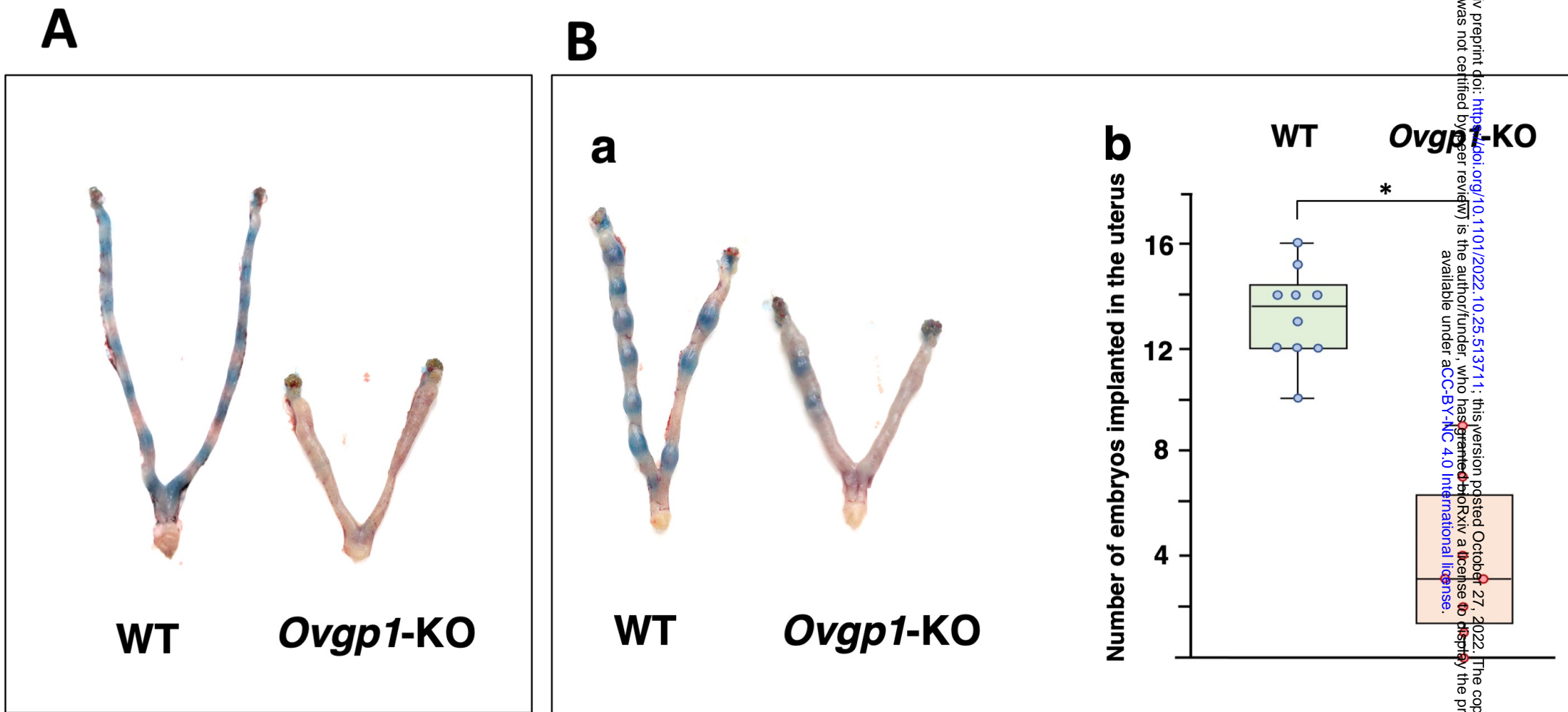


Figure 2.

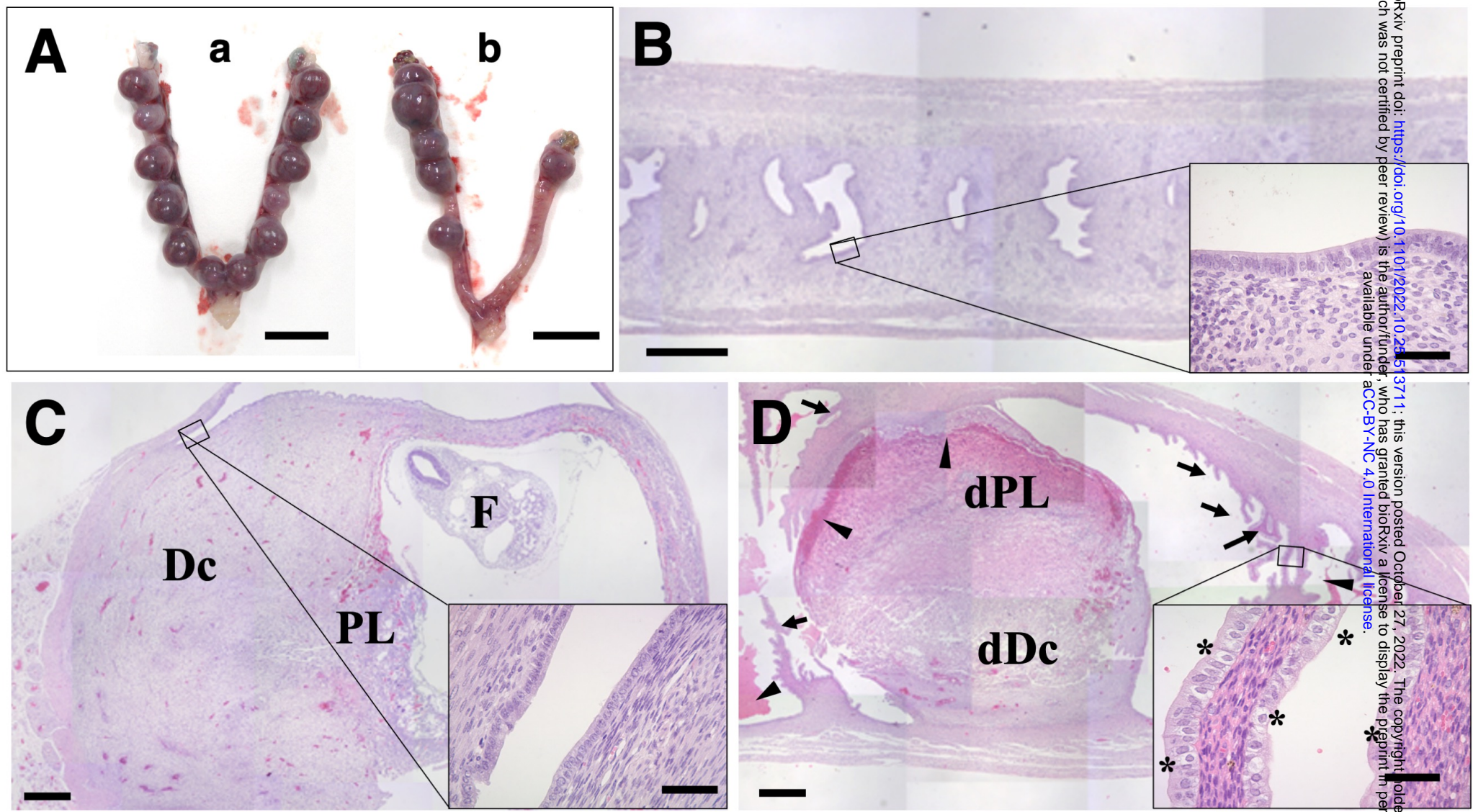
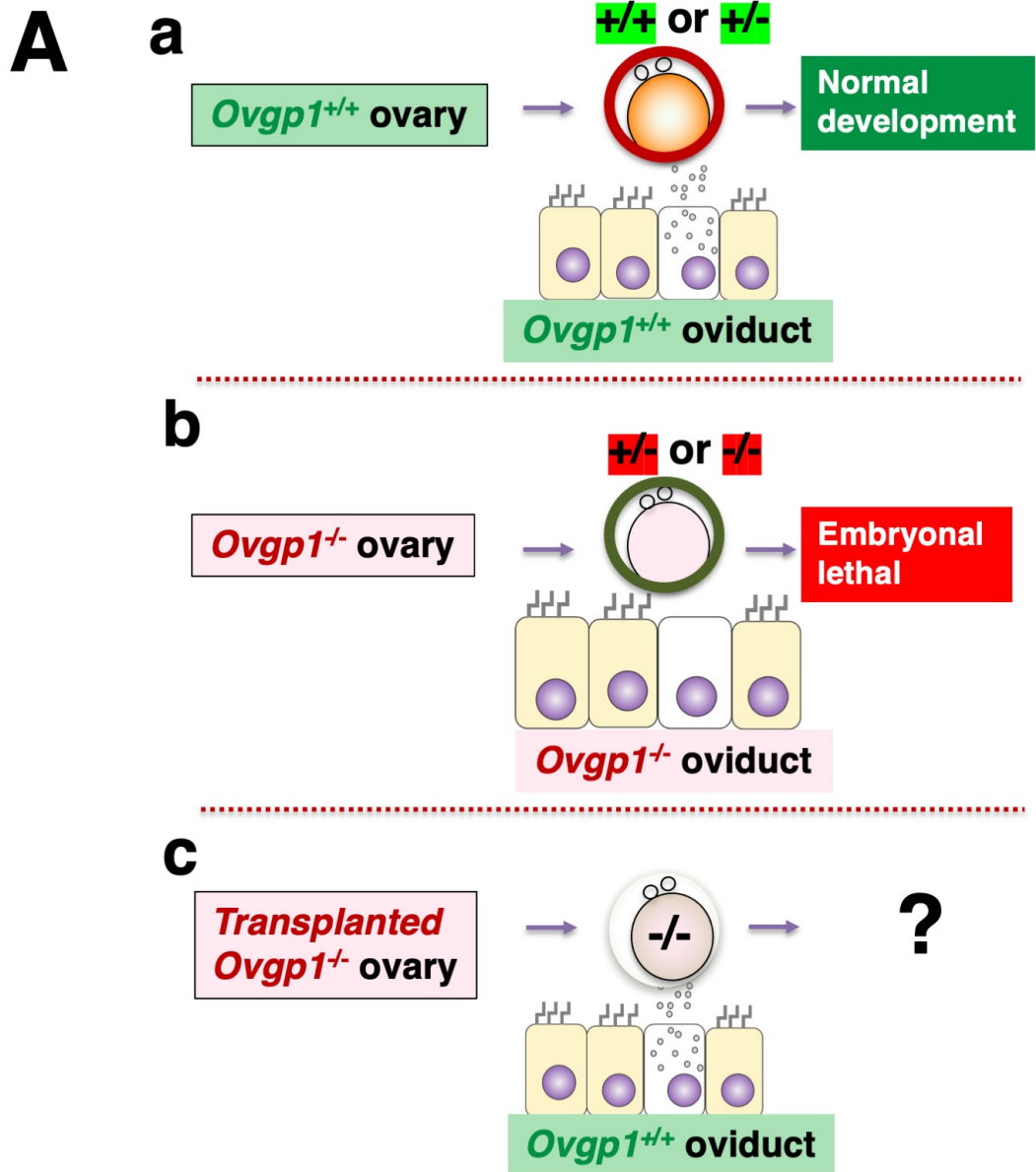
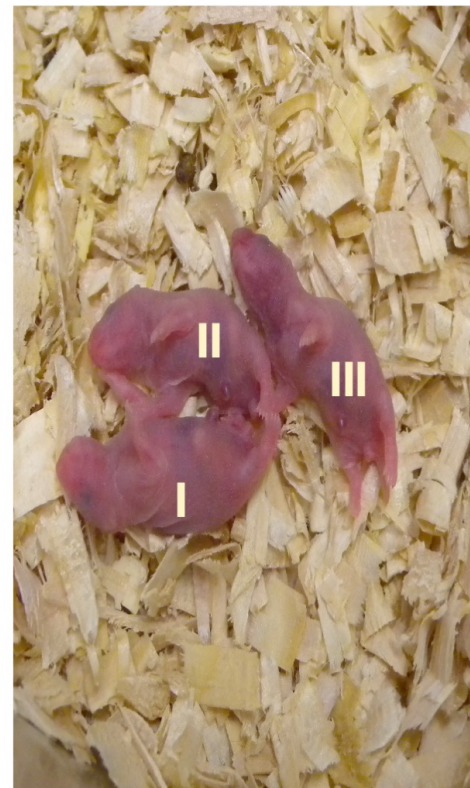


Figure 3.



B

a



b

I II III



Figure 4.

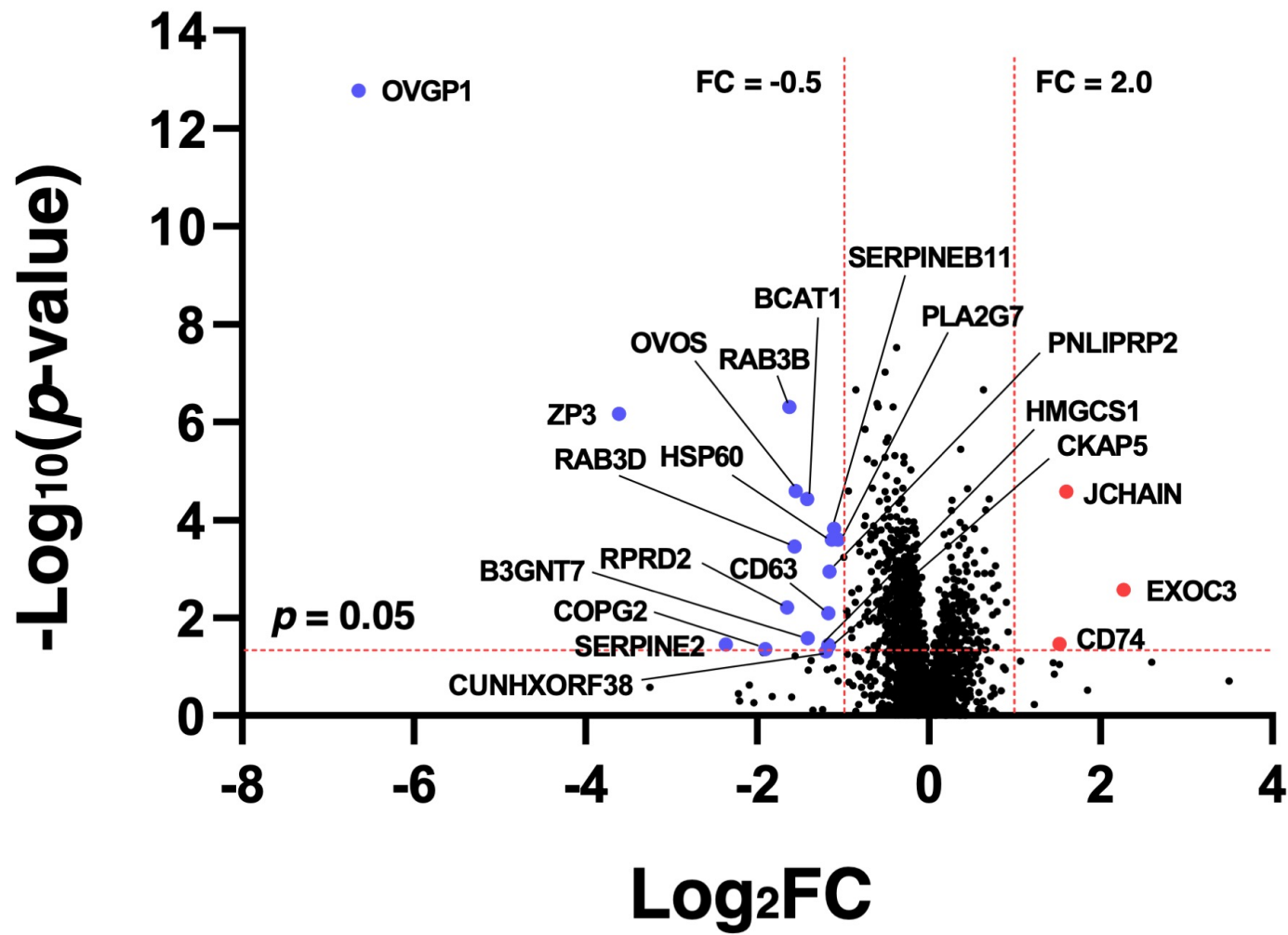


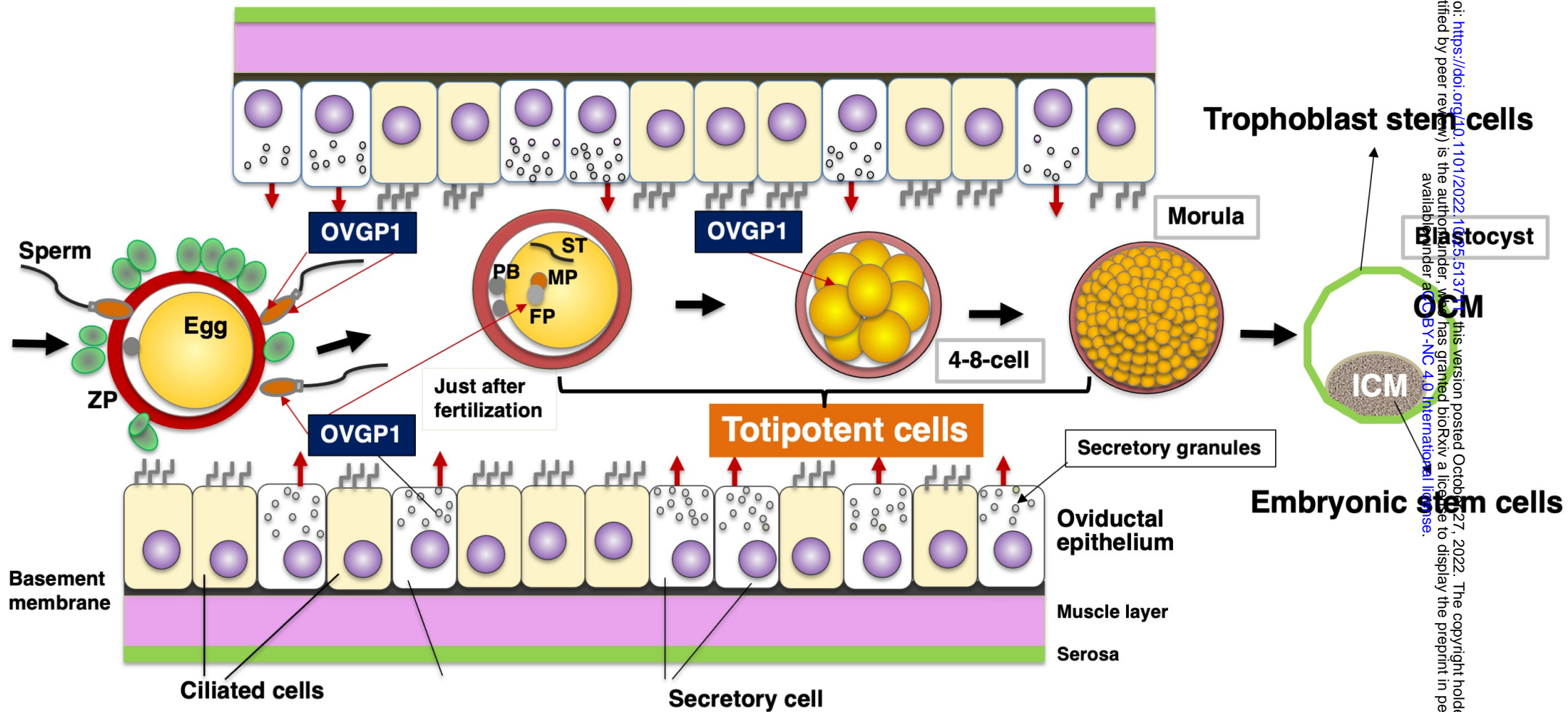
Figure 5.

Capacitation ↑
Acrosome Reaction ↑

Penetration ↑
Fertilization rate ↑
Polyspermy ↓

Cleavage effects ↑
Incorporated into the embryo ↑

Blastocyst formation ↑
Implantation ↑



bioRxiv preprint doi: <https://doi.org/10.1101/2022.10.25.513771>; this version posted October 27, 2022. The copyright holder for this preprint (which was not certified by peer review) is the author/funder, who has granted bioRxiv a license to display the preprint in perpetuity. It is made available under aCC-BY-NC 4.0 International license.

Figure 6.